HIGH POWER LASER
SCIENCE AND ENGINEERING

RESEARCH ARTICLE

Temporal-filtering dissipative soliton in an optical parametric oscillator

Hui Tong[1,†], Fuyong Wang[1,2,†], Zhipeng Qin[1], Guoqiang Xie[1], and Liejia Qian[1]

[1] *School of Physics and Astronomy, Key Laboratory for Laser Plasmas (Ministry of Education), Collaborative Innovation Center of IFSA (CICIFSA), Shanghai Jiao Tong University, Shanghai 200240, China*

[2] *School of Information and Electrical Engineering, Hebei University of Engineering, Handan 056038, China*

Abstract

Dissipative solitons have been realized in mode-locked fiber lasers in the theoretical framework of the Ginzburg–Landau equation and have significantly improved the pulse energy and peak power levels of such lasers. It is interesting to explore whether dissipative solitons exist in optical parametric oscillators in the framework of three-wave coupling equations in order to substantially increase the performance of optical parametric oscillators. Here, we demonstrate a temporal-filtering dissipative soliton in a synchronously pumped optical parametric oscillator. The temporal-gain filtering of the pump pulse combined with strong cascading nonlinearity and dispersion in the optical parametric oscillator enables the generation of a broad spectrum with a nearly linear chirp; consequently, a significantly compressed pulse and high peak power can be realized after dechirping outside the cavity. Furthermore, we realized, for the first time, dissipative solitons in an optical system with a negative nonlinear phase shift and anomalous dispersion, extending the parameter region of dissipative solitons. The findings may open a new research block for dissipative solitons and provide new opportunities for mid-infrared ultrafast science.

1. Introduction

Dissipative solitons are localized wavepackets of an electromagnetic field that are balanced through an energy exchange with the environment while nonlinearity and dispersion are involved[1]. In the theoretical framework of the Ginzburg–Landau equation, dissipative solitons have been realized in mode-locked lasers and have significantly improved the pulse energy and peak power levels of ultrashort pulse fiber lasers[1–15]. The formation of dissipative solitons in mode-locked fiber lasers is the result of a dynamic balance between the gain and spectral filtering loss with the interactions of dispersion and nonlinearity[1]. Based on numerical and experimental studies, dissipative soliton resonance[16–21], coexisting dissipative solitons[22] and breathing dissipative

soliton explosions[23,24] have been observed in mode-locked fiber lasers. The concept of dissipative solitons has promoted mode-locked fiber lasers to produce more powerful ultrashort laser pulses, which are vital for ultrafast science and industrial applications.

Optical parametric oscillators (OPOs) are of great interest as a source of broadly tunable ultrashort pulses from the ultraviolet to mid-infrared[25–32]. OPOs are in the framework of three-wave coupling equations, in which the gain is provided by a parametric conversion from the pump to the signal and idler. In addition, dispersion commonly exists in the OPO cavity, and a significant nonlinearity can be introduced by cascading nonlinear processes in the OPO cavity[33]. Accordingly, it is interesting to explore whether dissipative solitons can be formed in OPOs, and exploring dissipative solitons may substantially increase the performance of OPOs. In 2016, we proposed that broadband chirped pulses could be generated in an OPO while introducing nonlinearity in the cavity[34]. In 2018, Liu and Zhang[35] further demonstrated chirped pulse OPOs by introducing a material

---

Correspondence to: G. Xie, School of Physics and Astronomy, Key Laboratory for Laser Plasmas (Ministry of Education), Collaborative Innovation Center of IFSA (CICIFSA), Shanghai Jiao Tong University, Shanghai 200240, China. Email: xiegq@sjtu.edu.cn

†These authors contributed equally to this work.

1
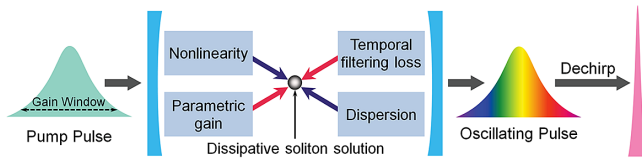
Figure 1. Schematic model of a temporal-filtering dissipative soliton in an OPO.

with a large nonlinearity in the cavity. In addition, spectra with steep edges were observed in a normal-dispersion fiber OPO[36] and a normal-dispersion fiber-feedback OPO[37], respectively. These works laid the foundation for the observation of dissipative solitons in OPOs.

In this study, we demonstrate that a temporal-filtering dissipative soliton can be formed in an OPO. When the system parameters in the OPO cavity enter a certain region, the temporal-gain-filtering effect of the pump pulse leads to the formation of a dissipative soliton with a broad spectrum and a nearly linear chirp. After dechirping outside the cavity, the pulse duration can be significantly compressed, and the peak power can be increased. Moreover, we demonstrate that temporal-filtering dissipative solitons can be formed not only in the normal-dispersion region with positive nonlinearity, but also in an anomalous-dispersion region with negative nonlinearity, which expands the parameter space in which the dissipative solitons exist.

2. Theoretical model of temporal-filtering dissipative soliton

Figure 1 shows a schematic model of the temporal-filtering dissipative soliton in an OPO. The gain of the optical parametric process is time-dependent, leading to a temporal window of the gain. Only the signal within this temporal window can be amplified, while the signal beyond this temporal window is lost, resulting in a temporal-filtering effect. A cascading nonlinearity supplied by the phase-mismatching second harmonic generation (SHG) of the oscillating pulse is introduced into the cavity to broaden the pulse spectrum. The nonlinear phase shift provided by the cascading nonlinearity of the SHG process can be calculated using the following expression[38]:

$$\Delta\varphi^{\mathrm{NL}} = -\alpha \frac{IL}{\Delta k},\qquad(1)$$

where α is a parameter related to the nonlinear coefficient. Thus, the nonlinear phase shift can be adjusted by regulating the intensity of the oscillating pulse I, wavevector mismatch Δk or nonlinear crystal length L. In addition, the third-order nonlinear effect of optical media can also provide a nonlinear phase shift. Moreover, an additional dispersion management element is required to control the net dispersion

in the cavity. When the parametric gain, temporal filtering loss, nonlinearity and dispersion in the OPO reach a dynamic balance, the oscillating pulse evolves into a dissipative soliton with a broad spectrum and a nearly linear chirp. The dissipative soliton can be dechirped outside the cavity, producing a significantly compressed pulse with a high peak power.

Numerical simulations were conducted to reveal the formation dynamics of the temporal-filtering dissipative solitons in the OPO. Detailed numerical simulation of the temporal-filtering dissipative soliton in the OPO is introduced in Section 1 of the Supplementary Material. Figure 2 shows the simulation results. The nonlinear phase shift mainly provided by the cascading nonlinearity generates new frequency components. The intracavity dispersion with the same sign as that of the nonlinear phase shift in the cavity temporally separates those frequency components, forming an approximately linear chirp in the pulse, as shown in Figure 2(a). The temporal separation between the frequencies increases with the value of the net intracavity dispersion; consequently, the slope of the linear chirp of the oscillating pulse decreases with the increase in the net intracavity dispersion. As new frequencies are generated and temporally separated, some of the frequency components go beyond the temporal-gain window and will be filtered, forming a temporal filtering effect in the OPO. Because the frequencies outside the temporal-gain window are cut off, the spectra of the dissipative solitons have characteristic steep edges (Figure 2(b)). As the dispersion decreases, the temporal separation between the frequencies decreases, and a wider frequency range can be accommodated in the temporal-gain window; thus, the output spectra of the dissipative solitons become wider. Finally, the dissipative soliton collapses when the intracavity dispersion is too small (see Section 2 of the Supplementary Material). Owing to its wide spectrum and nearly linear chirp, the dissipative soliton can be compressed outside the cavity. With the decrease in the intracavity dispersion, the spectrum of the dissipative soliton becomes wider; thus, the compressed pulse duration decreases (Figure 2(c)). Therefore, the pulse peak power after dechirping increases rapidly with a decrease in the intracavity dispersion (Figure 2(d)), indicating the potential of peak power scaling.

3. Experimental demonstration of a temporal-filtering dissipative soliton

An OPO setup was designed and built to demonstrate the temporal-filtering dissipative soliton, as shown in Figure 3. The OPO was synchronously pumped using a Yb-fiber-based main oscillator power amplifier system with a maximum output power of 60 W, a pulse duration of 800 fs and a repetition rate of 84.2 MHz at 1030 nm. The OPO cavity was designed to have two focus positions. Two magnesium
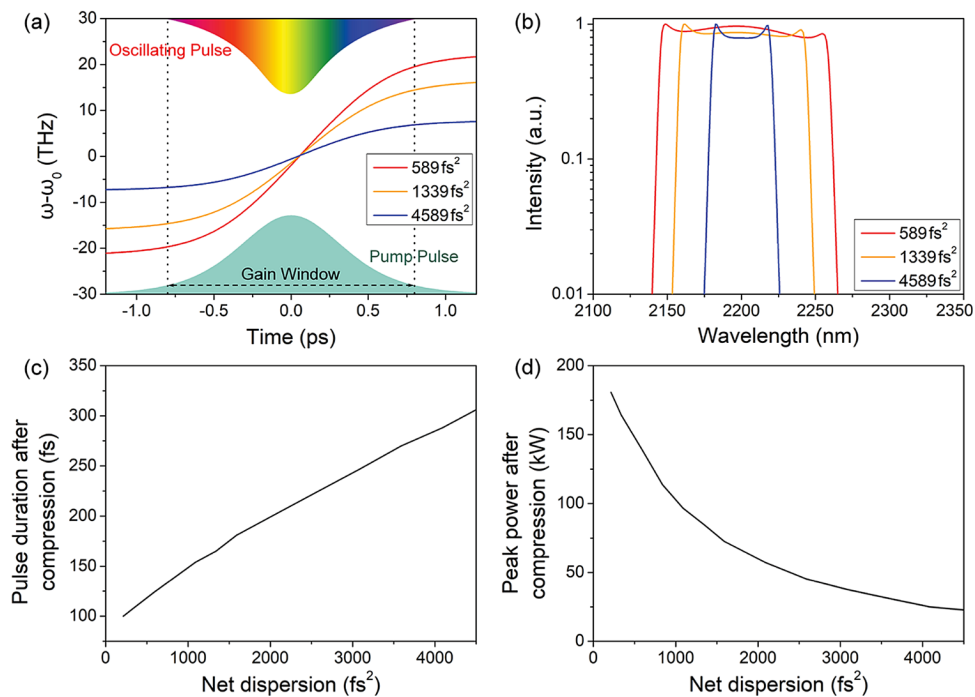
Figure 2. Numerical simulation results of a temporal-filtering dissipative soliton in the OPO. (a) Schematic of temporal-gain filtering and pulse chirp traces under different intracavity dispersions. (b) Spectra of dissipative solitons under different intracavity dispersions. (c) Pulse duration after compression versus intracavity dispersion. (d) Pulse peak power after compression versus intracavity dispersion.
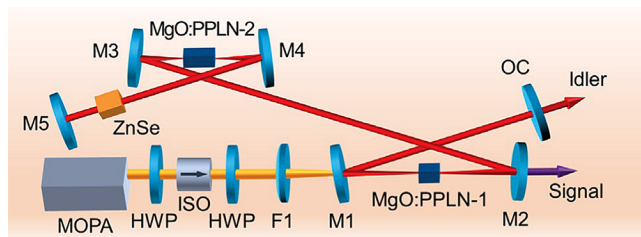

Figure 3. Experimental setup of the temporal-filtering dissipative soliton OPO. MOPA, Yb-fiber-based main oscillator power amplifier; HWP, half-wave plate; ISO, isolator; F1, plano-convex lens with a focal length of 300 mm; M1, M2, plano-concave mirrors with the same radius of curvature of 300 mm; M3, M4, plano-concave mirrors with the same radius of curvature of 100 mm; M5, plano-plano mirror. M1, M2, M3, M4 and M5 have a high reflectivity of more than 99.5% from 2.05 to 2.6 μm. OC, output coupler with a transmission of 3%. MgO:PPLN-1, MgO:PPLN-2 and ZnSe crystals are coated with a high transmission of more than 99.5% from 2.05 to 2.6 μm. The group velocity dispersions of ZnSe and MgO:PPLN are approximately 250 and −91 fs²/mm at 2.2 μm, respectively.

oxide-doped periodically poled lithium niobate (MgO:PPLN) crystals with the same polarization period of 31 μm were placed at two focal points. MgO:PPLN-1 with a length of 1.5 mm served as an OPO nonlinear crystal to provide the gain. MgO:PPLN-2 with a length of 3 mm was used as the cascading SHG crystal to produce a nonlinear phase shift. Zinc selenide (ZnSe) crystals of different lengths were used to regulate the net dispersion in the cavity.

In the experiment, the intracavity dispersion was introduced using a ZnSe crystal and two MgO:PPLN crystals.

ZnSe crystals with lengths of 4, 5, 6, 7 and 8 mm were used to control the net intracavity dispersion, corresponding to net intracavity dispersions of 589, 839, 1089, 1338 and 1588 fs², respectively. Figure 4(a) shows the output spectra of the idler for different intracavity dispersions. The idler pulses have wide spectra with steep edges, in good agreement with the simulation result shown in Figure 2(b). The wide spectra can be mainly attributed to the cascading nonlinear effect produced by the phase-mismatching SHG process of the idler in MgO:PPLN-2. At the back of M3 and M4 mirrors, the SHG of the idler with a central wavelength of 1.1 μm can be detected. With the MgO:PPLN-2 crystal with a polarization period of 31 μm, the wavevector mismatch of the SHG process of the idler was calculated to be -13.4 mm^{-1}. The calculated single-pass nonlinear phase shift provided by the cascading nonlinearity is 0.55π for the idler. In addition, the third-order nonlinearity of the MgO:PPLN-2 crystal provides a single-pass nonlinear phase shift of 0.12π, while the nonlinearity of the MgO:PPLN-1 crystal can be neglected due to a large beam size. Therefore, the total single-pass nonlinear phase shift is 0.67π, which causes significant spectrum broadening. In fact, we tried to draw out the MgO:PPLN-2 crystal from the optical path in the experiment, and the output spectrum became very narrow (~10 nm). In addition, the spectrum became wider as the net dispersion decreased. While the cavity has little net dispersion, more frequency components can be accommodated in the temporal-gain window, allowing a wider spectrum to oscillate in the cavity. When the net intracavity dispersion
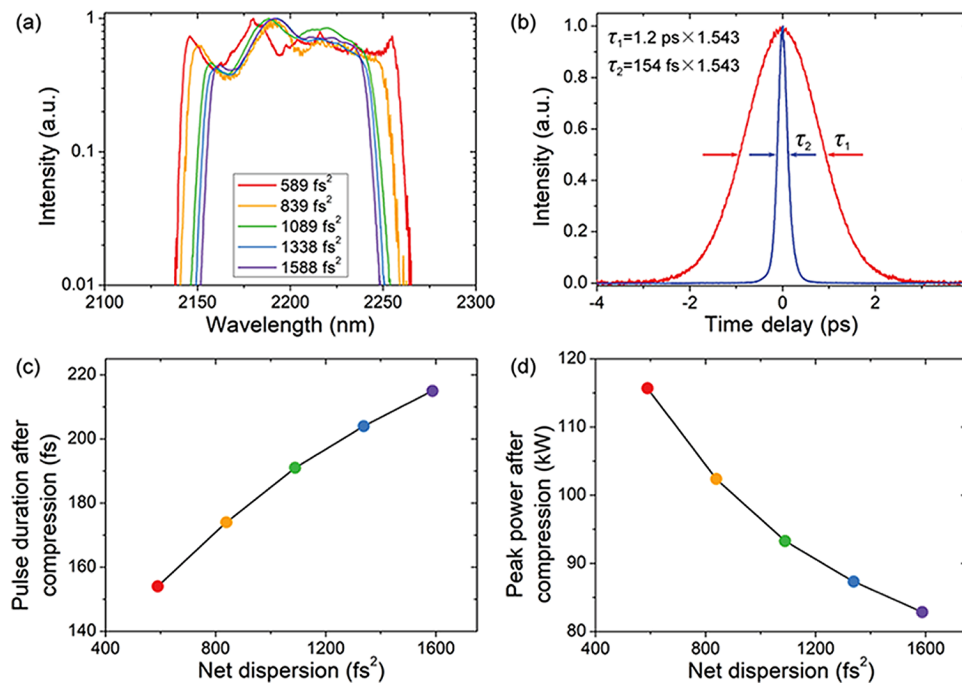
Figure 4. Experimental results of temporal-filtering dissipative soliton in an OPO. (a) Dissipative soliton spectra under different intracavity dispersions. (b) Autocorrelation traces of the output pulses before (red line) and after (blue line) compression when the intracavity dispersion is 589 fs^2. (c) Pulse duration after compression versus intracavity dispersion. (d) Pulse peak power after compression versus intracavity dispersion. The data are recorded at an average output power of 1.5 W.

is 589 fs^2, the spectrum has a maximum width of 127 nm (bandwidth of -20 dB). Notably, when the net intracavity dispersion is further reduced, the dissipative soliton in the cavity collapses. Therefore, dispersion is a key parameter for the formation of temporal-filtering dissipative solitons, and controlling the amount of net intracavity dispersion is important for achieving broadband dissipative solitons in the OPO.

The temporal-gain window is determined by the pump pulse duration; therefore, there is no significant difference in the pulse duration of the dissipative soliton under different values of the net intracavity dispersion. The output pulse has a full width at half maximum (FWHM) of 1.2 ps assuming a sech^2 profile, as shown in Figure 4(b). This dissipative soliton was compressed outside the cavity through two pairs of germanium prisms. Under a net intracavity dispersion of 589 fs^2, the chirped dissipative soliton can be compressed to 154 fs with a compression ratio of approximately 8. With the decrease in the net intracavity dispersion, the compressed pulse duration becomes narrower owing to the broadening of the spectrum of the dissipative soliton, and the peak power of the compressed pulse accordingly increases, as shown in Figures 4(c) and 4(d). The variation of the compressed pulse duration and peak power with intracavity dispersion is in basic agreement with the numerical simulation results in Figures 2(c) and 2(d), and the few differences might be caused by small dispersion of the cavity mirrors, which was neglected in the simulation. The temporal-filtering

dissipative soliton in the OPO is experimentally demonstrated, as shown in Figure 4, which can help to compress the pulse and promote the peak power of OPOs.

4. Formation conditions for a temporal-filtering dissipative soliton

To generate temporal-filtering dissipative solitons in an OPO, the nonlinear phase shift sign and dispersion sign play a key role. As expressed in Equation (1), the sign of the nonlinear phase shift $\Delta\varphi^{\mathrm{NL}}$ generated by the cascading nonlinearity can be switched by changing the sign of the wavevector mismatch Δk. Moreover, the sign of the net dispersion in the cavity can be regulated by employing ZnSe with different lengths. Based on the scheme above, the output characteristics of the idler under four different combinations of the positive/negative nonlinear phase shifts and normal/anomalous dispersions were experimentally studied; Figure 5 shows the results. For the two cases of the positive nonlinear phase shift combined with anomalous dispersion and the negative nonlinear phase shift combined with normal dispersion (Figures 5(b) and 5(d)), the output spectra are chaotic and unstable, which indicates that temporal-filtering dissipative solitons cannot be formed if the nonlinear phase shift and dispersion have opposite signs. When the signs of the nonlinear phase shift and dispersion are opposite, the oscillating pulse is compressed in the cavity owing to the interaction between the nonlinear spectral
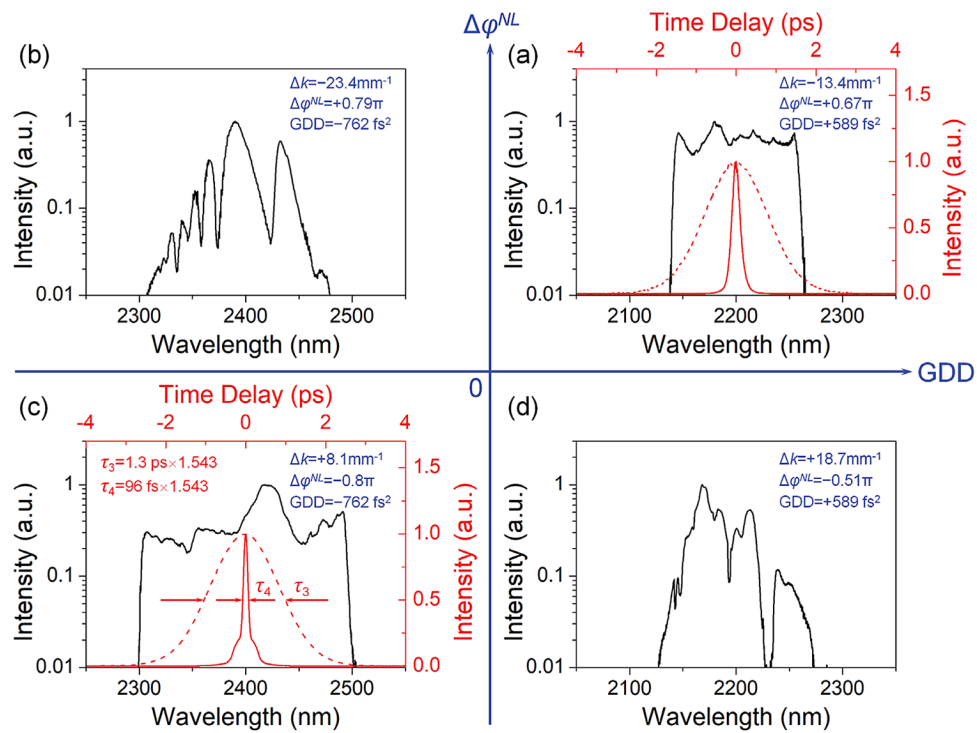
Figure 5. Output results of the OPO for four different combinations of positive/negative nonlinear phase shift and normal/anomalous dispersion. Black line, spectra of the idler; red dash line, autocorrelation traces of pulses before compression; red solid line, autocorrelation traces of pulses after compression; Δk, wavevector mismatch of the SHG process of the idler; $\Delta\varphi^{NL}$, single-pass nonlinear phase shift; GDD, net intracavity dispersion. (a), (c) Dissipative solitons. (b), (d) Collapsed solitons. In the OPO setup, the polarization periods of MgO:PPLN-2 are selected to be 31 μm for (a) and (b) and 36 μm for (c) and (d) to provide positive and negative nonlinear phase shifts, respectively. The length of the ZnSe crystal is set to 4 mm for (a) and (d) and no ZnSe crystal is inserted for (b) and (c) to realize normal and anomalous intracavity dispersions, respectively.

broadening and dispersion. In this case, almost no frequency components of the oscillating pulse go outside the temporal-gain window; thus, no temporal-filtering effect arises, and a dissipative soliton cannot be formed. At this time, the oscillating pulse generally operates as a conventional soliton under a small nonlinear phase shift and collapses when the nonlinear phase shift is accumulated to a certain extent.

The results shown in Figure 4 demonstrate that a temporal-filtering dissipative soliton can be formed for a positive nonlinear phase shift and normal dispersion. We further investigate the case of a negative nonlinear phase shift combined with an anomalous dispersion, as shown in Figure 5(c). In the experiment, we employed a MgO:PPLN-2 crystal with a polarization period of 36 μm, resulting in a wavevector mismatch of 8.1 mm^{-1} and a single-pass nonlinear phase shift of -0.93π. In addition, the single-pass nonlinear phase shift provided by the third-order nonlinearity of the MgO:PPLN-2 crystal is calculated to be $+0.13\pi$; thus, the total single-pass nonlinear phase shift is -0.8π. The intracavity dispersion was -762 fs^2 at 2.4 μm without inserting the ZnSe crystal. The OPO was tuned to 2.4 μm by adjusting the cavity length for stable operation because it collapsed at 2.2 μm for the large nonlinear phase shift and too little anomalous dispersion (-412 fs^2 at 2.2 μm). The output pulse has a wide

spectrum with steep edges, and the pulse duration is 1.3 ps assuming a sech^2 profile. The output pulse was dechirped by a germanium rod with a length of 12 mm (providing a dispersion of 2.77×10^4 fs^2)[39] and compressed to 96 fs with a compression ratio of approximately 14. The results indicate that a temporal-filtering dissipative soliton is also formed for the negative nonlinear phase shift and anomalous dispersion. Therefore, if we maintain consistent signs of the nonlinear phase shift and dispersion, the temporal-filtering dissipative soliton can be formed not only in the normal-dispersion region but also in the anomalous-dispersion region. This is the first time that a dissipative soliton in an optical system with a negative nonlinear phase shift and anomalous dispersion, which extends the parameter region of the dissipative soliton, has been realized. Because nonlinear crystals have generally anomalous dispersion in the mid-infrared region, a dissipative soliton with a negative nonlinear phase shift and anomalous dispersion may be a common phenomenon and it will be helpful to promote the level of mid-infrared ultrafast OPOs.

From the investigation above, we found that the formation of temporal-filtering dissipative solitons in OPOs relies on the interplay between the parametric gain, temporal-filtering loss, dispersion and nonlinearity in the cavity. The pump pulse provides a time-dependent gain, which forms a

temporal-gain window. The nonlinearity is responsible for producing new frequencies and broadening the spectrum. The dispersion temporally separates these frequencies and stretches the pulses. When some of the frequency components go outside the temporal-gain window, a temporal-gain-filtering effect occurs. Once the gain is balanced with the filtering loss, a dissipative soliton is formed in the OPO. If the nonlinearity is too small, few new frequencies will be generated. If the dispersion is too small, the pulse stretching will be very small. If the nonlinearity and dispersion have opposite signs, the oscillating pulse will be compressed but not stretched in the cavity. The above cases will not cause temporal-filtering effects. Therefore, a certain amount of nonlinearity and dispersion with the same sign is necessary for the formation of dissipative solitons in an OPO.

5. Conclusion

In conclusion, a temporal-filtering dissipative soliton is demonstrated in an OPO in the framework of three-wave coupling equations. The dissipative soliton in the OPO originates from the balance between the parametric gain and temporal-filtering loss through the interplay of nonlinearity and dispersion. Because of the temporal-filtering effect, the dissipative soliton in the OPO can generate a wide spectrum with a nearly linear chirp; thus, the pulse width can be significantly compressed, and the peak power can be increased after dechirping outside the cavity. In the experiment, we realized mid-infrared pulse compression up to 14-fold. Furthermore, we found that the temporal-filtering dissipative soliton can be formed only if the nonlinearity and dispersion in the optical systems have the same sign, and first realized a dissipative soliton in the region of anomalous dispersion and negative nonlinearity. The temporal-filtering dissipative soliton can support the generation of ultrashort femtosecond pulses pumped by long pulses, which promotes the stability of ultrafast OPOs. The finding of the temporal-filtering dissipative soliton opens a new research block of dissipative solitons and may have far-reaching implications for the development of mid-infrared OPOs.

Acknowledgments

Supplementary Materials

To view supplementary material for this article, please visit http://doi.org/10.1017/hpl.2022.6.

References

1. P. Grelu and N. Akhmediev, Nat. Photonics **6**, 84 (2012).
2. A. Chong, J. Buckley, W. Renninger, and F. Wise, Opt. Express **14**, 10095 (2006).
3. L. Zhao, D. Tang, and J. Wu, Opt. Lett. **31**, 1788 (2006).
4. B. Ortaç, O. Schmidt, T. Schreiber, and J. Limpert, Opt. Express **15**, 10725 (2007).
5. A. Chong, W. H. Renninger, and F. W. Wise, Opt. Lett. **32**, 2408 (2007).
6. C. Lecaplain, C. Chédot, A. Hideur, B. Ortaç, and J. Limpert, Opt. Lett. **32**, 2738 (2007).
7. W. H. Renninger, A. Chong, and F. W. Wise, Phys. Rev. A **77**, 023814 (2008).
8. A. Cabasse, B. Ortaç, G. Martel, A. Hideur, and J. Limpert, Opt. Express **16**, 19322 (2008).
9. K. Kieu, W. H. Renninger, A. Chong, and F. W. Wise, Opt. Lett. **34**, 593 (2009).
10. B. Ortaç, M. Baumgartl, J. Limpert, and A. Tünnermann, Opt. Lett. **34**, 1585 (2009).
11. S. Lefrançois, K. Kieu, Y. Deng, J. D. Kafka, and F. W. Wise, Opt. Lett. **35**, 1569 (2010).
12. M. Baumgartl, B. Ortaç, C. Lecaplain, A. Hideur, J. Limpert, and A. Tünnermann, Opt. Lett. **35**, 2311 (2010).
13. L. Zhao, D. Tang, X. Wu, and H. Zhang, Opt. Lett. **35**, 2756 (2010).
14. N. B. Chichkov, K. Hausmann, D. Wandt, U. Morgner, J. Neumann, and D. Kracht, Opt. Lett. **35**, 2807 (2010).
15. L. Zhao, D. Tang, H. Zhang, X. Wu, Q. Bao, and K. Loh, Opt. Lett. **35**, 3622 (2010).
16. W. Chang, A. Ankiewicz, J. M. Soto-Crespo, and N. Akhmediev, Phys. Rev. A **78**, 023830 (2008).
17. W. Chang, J. M. Soto-Crespo, A. Ankiewicz, and N. Akhmediev, Phys. Rev. A **79**, 033840 (2009).
18. X. Wu, D. Y. Tang, H. Zhang, and L. M. Zhao, Opt. Express **17**, 5580 (2009).
19. P. Grelu, W. Chang, A. Ankiewicz, J. M. Soto-Crespo, and N. Akhmediev, J. Opt. Soc. Am. B **27**, 2336 (2010).
20. E. Ding, P. Grelu, and J. N. Kutz, Opt. Lett. **36**, 1146 (2011).
21. L. Duan, X. Liu, D. Mao, L. Wang, and G. Wang, Opt. Express **20**, 265 (2012).
22. C. Bao, W. Chang, C. Yang, N. Akhmediev, and S. T. Cundiff, Phys. Rev. Lett. **115**, 253903 (2015).
23. J. Peng and H. Zeng, Phys. Rev. Appl. **12**, 034052 (2019).
24. Y. Zhou, Y.-X. Ren, J. Shi, and K. K. Y. Wong, Photon. Res. **8**, 1566 (2020).
25. M. Ghotbi, A. Esteban-Martin, and M. Ebrahim-Zadeh, Opt. Lett. **33**, 345 (2008).
26. M. A. Watson, M. V. O'Connor, D. P. Shepherd, and D. C. Hanna, Opt. Lett. **28**, 1957 (2003).
27. J. B. Dherbecourt, A. Godard, M. Raybaut, J. M. Melkonian, and M. Lefebvre, Opt. Lett. **35**, 2197 (2010).
28. L. Maidment, P. G. Schunemann, and D. T. Reid, Opt. Lett. **41**, 4261 (2016).
29. C. F. O'Donnell, S. C. Kumar, P. G. Schunemann, and M. Ebrahim-Zadeh, Opt. Lett. **44**, 4570 (2019).
30. H. Tong, G. Xie, Z. Qiao, Z. Qin, P. Yuan, J. Ma, and L. Qian, Opt. Lett. **45**, 989 (2020).
31. J. Fan, J. Zhao, L. Shi, N. Xiao, and M. Hu, Adv. Photonics **2**, 045001 (2020).
32. J. Wu, R. Su, A. Fieramosca, S. Ghosh, J. Zhao, T. C. H. Liew, and Q. Xiong, Adv. Photonics **3**, 055003 (2021).
33. I. Stasevičius and M. Vengris, Opt. Express **28**, 26122 (2020).
34. G. Xie, L. Qian, F. Wang, Z. Qin, and P. Yuan, "Method for generating ultrashort femtosecond pulses in optical parametric

oscillator pumped by long pulses," U. S. Patent 9,366,939 B2 (June 14, 2016).

35. P. Liu and Z. Zhang, Opt. Lett. **43**, 4735 (2018).
36. T. N. Nguyen, K. Kieu, A. V. Maslov, M. Miyawaki, and N. Peyghambarian, Opt. Lett. **38**, 3616 (2013).
37. C. F. O'Donnell, S. C. Kumar, T. Paoletta, and M. Ebrahim-Zadeh, Optica **7**, 426 (2020).
38. X. Liu, L. Qian, and F. Wise, Opt. Lett. **24**, 1777 (1999).
39. Z. Qin, G. Xie, H. Gu, T. Hai, P. Yuan, J. Ma, and L. Qian, Adv. Photonics **1**, 065001 (2019).